# The Stress State of Elastic Fluids in Viscometric Flow

**M. J. MILLER and E. B. CHRISTIANSEN**

**Department of Chemical Engineering**
**University of Utah, Salt Lake City, Utah 84112**

**A new method of instrumentation for normal-stress determinations was developed, making possible accurate unsteady state as well as steady state measurements, eliminating errors arising from fluid-filled pressure-tap holes, and permitting the determination of the complete stress state in a single cone-and-plate shearing-geometry experiment. Sensitive, nonflow semiconductor pressure transducers mounted at several radial positions with their pressure-sensing diaphragms flush with the plate surface provide data for the normal-stress distribution. The normal-stress distribution, together with the total normal force from the single-geometry experiment, enables determination of the primary and secondary normal-stress differences by two independent methods of analysis while the transmitted torque enables determination of the viscosity, each as a function of shear rate. Only the normal-stress distribution is required if an independent check on the normal-stress determination is not desired. Similar advantages arise in the application of the instrumentation to a parallel-plate shearing geometry. The new instrumentation was used in the determination of the complete rheological stress state of three aqueous and two "Tetralin" solutions of polymers in a cone-and-plate shearing geometry for shear rates of 0.02 to 450 $s^{-1}$ on a Model R-17 Weissenberg Rheogoniometer. The normal-stress differences computed by means of two methods of analysis are in surprisingly good agreement. The ratio of the secondary to the primary normal-stress difference was negative. The absolute values of this ratio decreased with increases in the shear rate, the maximum observed value being 0.4.**

During the past two decades, great interest has been expressed in both the theoretical and experimental aspects of simple shearing of elastic liquids. Although significant advances have been made in the mathematical formulation of constitutive or rheological equations of state, the experimental data available are not sufficiently precise nor complete to evaluate these models adequately. A critical need here is for more suitable experimental methods. The purpose of the presently reported research was to develop a more accurate experimental method and to provide more accurate, complete data on the primary and secondary normal-stress differences.

Data from experimental investigations in polymer-solution and -melt rheology are most easily interpreted when unidirectional or viscometric flows—such as those shown schematically in Figure 1—are used. The direction of flow is designated the "1" direction; the direction of the velocity gradient, the "2" direction; and the remaining orthogonal, or neutral, direction, the "3" direction. Hence, a viscometric flow field is described by the equations

$$V_1 = V_1(X_2), \quad V_2 = V_3 = 0 \tag{1}$$

where $V_i$ ($i = 1, 2, 3$) are the orthogonal components of the velocity vector and $X_2$ is a distance in the 2 direction.

For such a simple flow field, it can be shown from the existing symmetry (*27*) that the total-stress tensor $\sigma_{ij}$ ($i, j = 1, 2, 3$) possesses only four distinct nonzero components (the total-stress tensor is assumed to be symmetric):

$$\sigma_{ij} = \begin{bmatrix} \sigma_{11} & \sigma_{12} & 0 \\ \sigma_{21} & \sigma_{22} & 0 \\ 0 & 0 & \sigma_{33} \end{bmatrix}. \tag{2}$$

Correspondence concerning this paper should be addressed to E. B. Christiansen. M. J. Miller is now with the Eastman Kodak Company, Rochester, New York.

The diagonal terms $\sigma_{ii}$ ($i = 1, 2, 3$) are the normal-stress components; and the off-diagonal terms, $\sigma_{ij}$ ($i, j = 1, 2, 3$; $i \neq j$), are the shear-stress components.

The isotropic pressure $p$ is defined as one-third of the trace of the total-stress tensor (*8, 27, 40*):

$$p = \frac{1}{3}(\sigma_{11} + \sigma_{22} + \sigma_{33}) \tag{3}$$

This definition reduces to the hydrostatic pressure for nonelastic, incompressible Newtonian fluids. For viscoelastic fluids (characterized as having unequal normal-stress components), this definition is equal only to an average of the normal-stress components.

A shear-stress, or deviatoric-stress, tensor $\tau_{ij}$ is defined as (*8, 27, 40*):

$$\tau_{ij} = \sigma_{ij} - p\delta_{ij}, \tag{4}$$

where $\delta_{ij}$ is the unit tensor (Kronecker Delta). From Equations (3) and (4), it follows that

$$\tau_{11} + \tau_{22} + \tau_{33} = 0. \tag{5}$$

Only two of the three diagonal components of the shear-stress tensor are independent. Therefore, only three dynamic functions are of rheological importance in the description of the steady-viscometric-flow behavior of an elastic fluid (*27*):

$$\tau_{21}, \quad \tau_{11} - \tau_{22}, \quad \tau_{22} - \tau_{33} \tag{6}$$

(or any independent combination of the differences of the normal-stress components), where $\tau_{21}$ is the shear stress, $(\tau_{11} - \tau_{22})$ and $(\tau_{22} - \tau_{33})$ are the primary and secondary normal-stress differences $N_1$ and $N_2$ respectively.

Several investigations have been conducted to determine the complete stress state of a viscoelastic fluid undergoing simple shearing (*1, 4, 9, 13* to *15, 22, 25, 26, 30*). Some of the results of these investigations are given

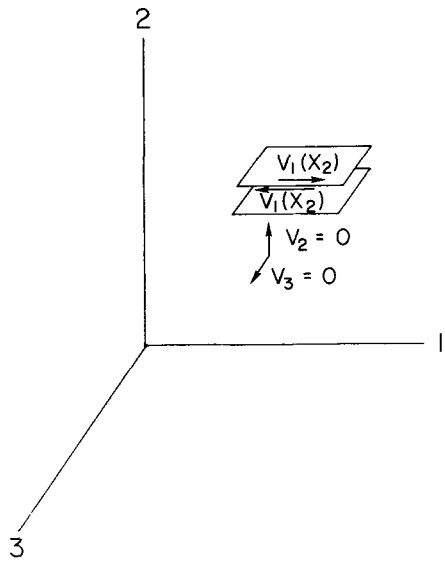


Fig. 1. Simple viscometric flow.

in Table 1. As can be seen from a comparison of these results, $N_2$ has been a difficult quantity to determine. Many of these studies suffer from the lack of precision in the establishment and maintenance of the appropriate boundary conditions. Some results [for example (*1*, *28*)] include the effects of "hole" errors (*25*) introduced by the use of test fluid to transmit pressure through holes in the wall of the flow system to the pressure sensor. However, "hole" errors are reported to be negligible in the case of polymer melts (*16*). In addition, some of the more recent studies (particularly, the annular-pipe-flow studies) suffer from inherent assumptions in employed constitutive equations or from the methods of data analysis; for example, the integral-inversion techniques (*17*, *38*). Weaknesses in some recent investigations have been described (*14*).

Sophisticated and reliable instrumentation which has become available in recent years has made possible a more meaningful determination of $N_1$ and $N_2$. It has been established (*17*) that the sign of $N_1$ is negative (positive stresses signify compressive forces on an elemental volume of fluid); in addition most rheologists consider the Weissenberg hypothesis ($\tau_{22} = \tau_{33}$) to be invalid. However, experimental investigators have not generally agreed upon the sign of $N_2$ (see Table 1), its shear-rate dependence, or its relative magnitude (compared with $N_1$).

Recent results obtained from an instability analysis of Couette flow in a concentric-cylinder viscometer (*4*, *11*), from cone-and-plate data corrected for hole errors (*25*), from combined cone-and-plate data (*14*), and from some corrected previous data and channel-flow data (*39*) indicate that the sign of $N_2$ is opposite to that of $N_1$. The presently reported data—obtained by methods which eliminate hole errors which are more direct and which provide an independent check of data consistency not possible in previous methods—also indicate that $N_2$ represents a net compression.

## ANALYSIS OF THE CONE-AND-PLATE SHEAR DEVICE

The cone-and-plate shear generator provides a means for determining the total stress state of a viscoelastic fluid at relatively low shear rates with a minimum of uncertainty resulting from incorporated simplifying assumptions.

The idealized velocity field between the plate and cone surfaces can be described by

$$V_\phi = r\Omega \frac{\theta - \pi/2}{\theta_c - \pi/2} \tag{7}$$

where $r$, $\theta$ and $\phi$ are the polar spherical coordinates as shown in Figure 2; $\theta_c$ is the cone angle; and $\Omega$ is the angular velocity of the rotating cone. For the steady state shearing of an isotropic incompressible fluid, the $\phi$ component of the equation of motion can be reduced to

Table 1. Results of Several Investigations of the Complete Stress State of a Viscoelastic Liquid

| Investigator | Year | Shear device | Results[a] | Approximate shear rate, $sec^{-1}$ |
|---|---|---|---|---|
| Garner, Nissan, and Wood (*9*) | 1950 | Parallel plate | $\tau_{11} = \tau_{22} = \tau_{33} = 0$ | |
| Roberts (*35*) | 1952 | Cone and plate | $\tau_{22} = \tau_{33}$ | |
| Greensmith and Rivlin (*15*) | 1953 | Parallel plate | $\tau_{11} = \tau_{22}$ | |
| Pollett (*33*) | 1955 | Cone and plate | $\tau_{22} = \tau_{33}$ | |
| Kotaka, Kurata, and Tamura (*26*) | 1959 | Parallel plate | $\tau_{22} = \tau_{33}$ | |
| Sakiadis (*36*) | 1962 | Tube flow | $\tau_{22} - \tau_{33} < 0$ | |
| Markovitz and Brown (*28*) | 1963 | Cone and plate<br>Parallel plate | $\tau_{22} - \tau_{33} < 0$ | $<100$ |
| Adams and Lodge (*1*) | 1963 | Cone and plate<br>Parallel plate | $\tau_{22} - \tau_{33} < 0$ | |
| Ginn and Metzner (*13*) | 1965 | Cone and plate<br>Parallel plate | $\tau_{22} - \tau_{33} > 0$<br>$\tau_{22} - \tau_{33} = 0$ | $\leq 70$<br>$>70$ |
| Hayes and Tanner (*17*) | 1965 | Annular flow | $\tau_{22} - \tau_{33} < 0$ | |
| Huppler (*20*) | 1965 | Annular flow | $\tau_{22} - \tau_{33} < 0$ | $<1500$ |
| Jackson and Kaye (*22*) | 1966 | Cone and plate | $\tau_{22} - \tau_{33} > 0$ | $<3$ |
| Tanner (*38*) | 1967 | Annular flow | $\tau_{22} - \tau_{33} < 0$ | $<750$ |
| Huppler, Ashare, and Holmes (*21*) | 1967 | Cone and plate | $\tau_{22} - \tau_{33} < 0$ | |
| Kaye, Lodge, and Vale (*25*) | 1968 | Concentric cylinder<br>Cone and plate<br>Plate and plate | $\tau_{22} - \tau_{33} > 0$ | $<25$ |
| Ginn and Metzner (*14*) | 1969 | Cone and plate<br>Parallel plate | $\tau_{22} - \tau_{33} > 0$ | $<100$ |
| Denn and Roisman (*4*) | 1969 | Concentric cylinder | $\tau_{22} - \tau_{33} > 0$ | |
| Tanner (*39*) | 1970 | Inclined channel | $\tau_{22} - \tau_{33} > 0$ | low |

[a] Positive stresses are compressive in nature.

$$\frac{\partial \tau_{21}}{\partial \theta} + 2\,\tau_{21} \cot \theta = 0 \qquad (8)$$

where the notation for direction specification given above has been used. The solution to this equation (27) is

$$\tau_{21} = \frac{3\Gamma}{2\pi R^3} \qquad (9)$$

where $\Gamma$ is the torque transmitted through the fluid from the cone to the plate and $R$ is the radius of the plate and the cone.

The shear rate $\dot{\gamma}$ for the cone-and-plate velocity field is

$$\dot{\gamma} = \frac{\Omega}{\alpha}\,[1 - (\theta - \pi/2) \cot \theta] \qquad (10)$$

where $\alpha$ is the complementary cone angle $\theta_c - \pi/2$. If $\alpha$ is small (4° or less),

$$\dot{\gamma} \simeq \Omega/\alpha. \qquad (11)$$

The apparent viscosity $\eta$ can be calculated by use of Equations (9) and (11):

$$\eta \equiv \frac{\tau_{21}}{\dot{\gamma}} = \frac{3\Gamma\alpha}{2\pi R^3 \Omega} \qquad (12)$$

Two methods of analysis that employ the $r$ component of the equation of motion were used to determine $N_1$ and $N_2$: the rim-pressure method and the integral-force method. The $r$-component equation, upon simplification, becomes

$$\frac{\partial \sigma_{33}}{\partial r} = \frac{\partial p}{\partial r} + \frac{\partial \tau_{33}}{\partial r} = \frac{\tau_{11} + \tau_{22} - 2\tau_{33}}{r} \qquad (13)$$

Since $N_2$ can be shown to be a material function (27), this function can be differentiated with respect to spatial coordinates:

$$\frac{\partial \sigma_{22}}{\partial \ln r} - \frac{\partial \sigma_{33}}{\partial \ln r} = 0 \qquad (14)$$

A combination of Equations (13) and (14) provides the normal-stress gradient

$$\chi \equiv \frac{\partial \sigma_{22}}{\partial \ln r} = (\tau_{11} - \tau_{22}) - 2(\tau_{22} - \tau_{33}). \qquad (15)$$

### Rim-Pressure Method of Analysis

A force balance at the air-fluid interface (Figure 2) requires that the ambient pressure be equal to the normal stress $\sigma_{33}$ providing that the air-fluid interface is spherical in form (1, 27) and that centrifugal-force and surface-tension effects are negligible or corrected for. If the ambient pressure $p_A$ is taken as the zero reference of pressure,

$$\sigma_{33}(R) = p_A = 0 \qquad (16)$$

and

$$\tau_{22} - \tau_{33} = \sigma_{22}(R). \qquad (17)$$

Thus, $N_2$ can be calculated by determining the rim value of $\sigma_{22}$. Prior to this investigation, this technique had provided only questionable results (1, 15, 35).

From the slope of the $\sigma_{22}$ normal-stress distribution, $N_1$ can be calculated by use of Equations (15) and (17):

$$\tau_{11} - \tau_{22} = \chi - 2(\tau_{22} - \tau_{33}). \qquad (18)$$

Use of Equations (12), (17), and (18) permits calculation of the complete stress state of a viscoelastic fluid undergoing a simple viscometric flow. This technique is referred to as the rim-pressure method.

### Integral-Force Method of Analysis

The total stress state can be determined in an alternative manner introduced by Jobling (23), which involves the measurement of the total axial thrust generated within an elastic material sheared in a cone-and-plate device. The axial thrust $F$ is equal to the integral of the $\sigma_{22}$ normal-stress distribution over the area of the flat plate:

$$F = \int_0^{2\pi} \int_0^R [-\sigma_{22}(r)]r\,dr\,d\phi \qquad (19)$$

This integration can be performed by use of Equations (15) and (16), yielding

$$\tau_{11} - \tau_{22} = \frac{2F}{\pi R^2} \qquad (20)$$

If the local stress distribution $\sigma_{22}(r)$ is known, $N_2$ can be calculated by use of Equation (15)

$$\tau_{22} - \tau_{33} = \tfrac{1}{2}[\chi - (\tau_{11} - \tau_{22})]. \qquad (21)$$

Thus, the complete stress state of a viscoelastic fluid can be calculated as a function of shear rate by use of Equations (12), (20), and (21). This method is known as the integral-force, or total-thrust, method of analysis. It is also clear that the complete stress state can be determined by use of Equations (12), (17), and (20).

## APPARATUS

A shear generator capable of measuring simultaneously the transmitted torque, the total axial thrust, and local values of the $\sigma_{22}$ normal stress as a function of the shear rate was used in obtaining the data reported herein. The basic shearing device used was a Model R-17 Weissenberg Rheogoniometer. This rheometer was originally instrumented to measure only the transmitted torque and the total axial thrust as a function of shear rate. To obtain the normal-stress distribution $\sigma_{22}(r)$ five small fast-response semiconductor pressure transducers were mounted along a radial line of the plate, with the ⅛-in. O.D. flat pressure-sensing diaphragms flush with the plate surface in order to eliminate "hole" (25) and other errors (30). Although we (37) have been able to reduce hole errors experimentally in tube-flow measurements and others (25) have used measured corrections, the use of flush-mounted sensors is most promising.

The electrical-power dissipation per transducer was only about 0.07 watts, which should be negligible in its effect on fluid properties. The inherent uncertainty in pressure measurements was determined to be less than 130 dynes/cm², half

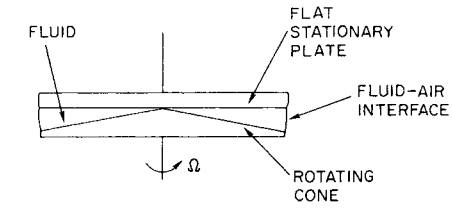


A. CONE-AND-PLATE GEOMETRY

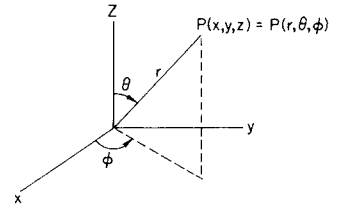


B. POLAR-SPHERICAL-COORDINATE SYSTEM

**Fig. 2. Cone-and-plate shearing geometry.**

the uncertainty specified by the manufacturer. This uncertainty may have been caused by friction in a mechanical linkage between the transducer diaphragms and semiconductor crystals. The effect of this relatively large uncertainty in pressure measurements was reduced by an appropriate choice of the fluids to be tested. The inherent uncertainty of the pressure transducers was less than the uncertainty in the recorder output for more than half of the measurements reported.

The stainless-steel cone-and-plate platens used were 100 mm in diameter. Two cones with angles of 1.921 and 3.972° were used. The platens were enclosed in a temperature-control chamber in which the temperature of the test fluid could be controlled within ±0.1°C. All rheological data presented herein were taken at 25.2 ± 0.1°C.

Continuous records of the transmitted torque, the total axial thrust, and the five values of the stress normal to the flat plate were obtained on a multichannel optical oscillograph. Each signal was amplified to a recordable level on a variable-gain differential amplifier (especially chosen for minimal noise introduction) prior to being circuited to the UV oscillograph. Since the fluid-damped optical galvanometers had a nominal frequency response of DC to 600 Hz and the frequency response of the pressure transducers was DC to 60 kHz, this system not only provided the steady state but also the complete transient response of the fluid to shearing. Only the steady state fluid response will be discussed in this paper. A qualitative description of the transient behavior has been reported elsewhere (*3, 30*).

## FLUIDS

Two solutions of Separan AP-30 (polyacrylamide, PAA) in a water-glycerine solvent, one aqueous solution of Polyox WSR-301 (polyethylene oxide, PEO), and two solutions of Vistanex L-140 (polyisobutylene, PIB) in Tetralin were tested on the modified Model R-17 Weissenberg Rheogoniometer. These polymer solutions were chosen for their stability and the large normal stresses generated during steady-shearing flow. Table 2 contains their compositions, measured physical properties, and known molecular parameters.

## EXPERIMENTAL RESULTS

The PAA solutions exhibited non-Newtonian viscosities over the five-decade range of shear rates covered. Figures 3 and 4 show the apparent viscosity and normal-stress differences, respectively, as a function of shear rate for the 1.49% PAA solution. The dependence of the normal-stress-difference ratio

$$\psi \equiv -N_2/N_1 \qquad (22)$$

on shear rate is shown in Figure 5. Contrary to the results of some data analysis (*20, 36*), this ratio is not constant but varies with the shear rate in qualitative agreement with the data of Ginn and Metzner (*11, 13*) and our computations based on the presentation by Kaye, Lodge, and Vale (25). It should be emphasized that the data presented in Figures 3, 4, and 5 were taken on two cones of 2 and 4° angles (nominal values). Shown for comparison are the data calculated by the integral-force and rim-pressure methods of analysis. The excellent agreement

TABLE 2. PROPERTIES OF THE POLYMER SOLUTIONS

| Polymer | Concentration, weight % | Solvent, weight % | Molecular weight |
|---|---|---|---|
| PAA (Separan AP-30) Dow Chemical | 1.00 | 50% water 50% glycerin | 2 to 3 ($10^6$)* |
| | 1.49 | 50% water 50% glycerin | 2 to 3 ($10^6$)* |
| PEO (Polyox WSR-301) Union Carbide | 3.54 | Water | 4 ($10^6$) |
| PIB (Vistanex L-140) Enjay Chemical | 4.17 | Tetralin | 2.1 to 2.6 ($10^6$) |
| | 7.30 | Tetralin | 2.1 to 2.6 ($10^6$) |

* Estimate of the Dow Chemical Company, Midland, Michigan.

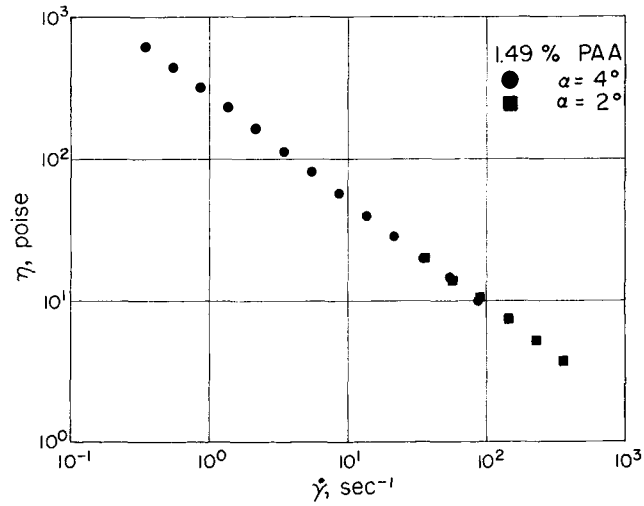


Fig. 3. Apparent viscosity as a function of shear rate for the 1.49% PAA solution.

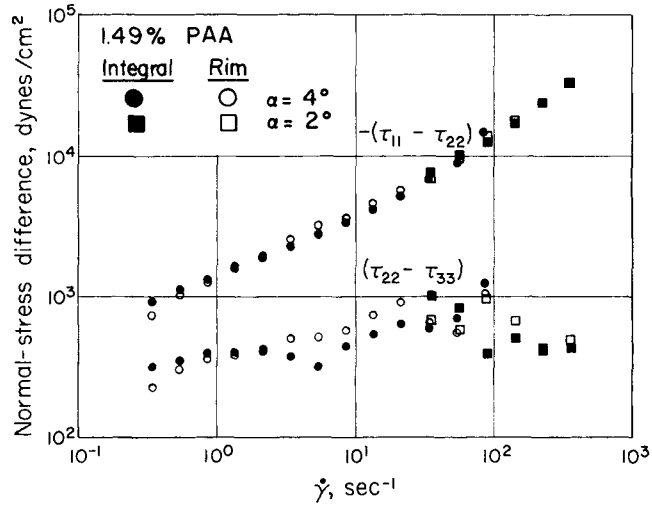


Fig. 4. Primary and secondary normal-stress differences as a function of shear rate for the 1.49% PAA solution, determined by means of the integral-force and rim-pressure methods.

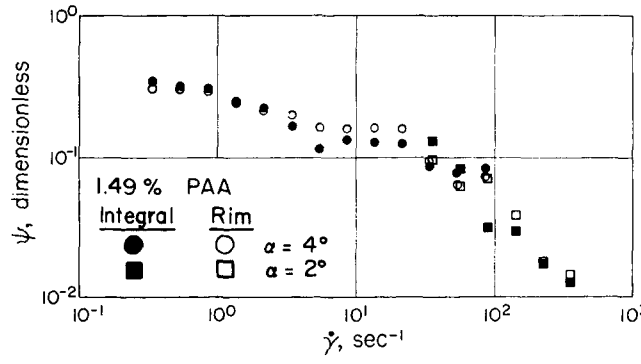


Fig. 5. Normal-stress-difference ratio, $\psi = N_2/N_1$, as a function of shear rate for the 1.49% PAA solution.

that was obtained using the integral-force and rim-pressure methods represents a precedent for such measurements [for example, (1)].

Also, the total axial thrust measured on the rheogoniometer $F_{rheo}$ was compared with the area integral of the measured normal-stress distribution. The normal-stress distribution $\sigma_{22}(r)$ was determined by fitting values of this stress at known radial positions by means of a linear least-squares technique to the equation

$$\sigma_{22}(r) = A + \chi \ln r \qquad (23)$$

where $r$ is the radial position of the center of the pressure transducer, $\chi$ is the slope of the logarithmic stress distribution [Equation (15)], and $A$ is the value of $\sigma_{22}$ at $r =$ 1 cm. Equation (23) was then integrated analytically:

$$F_D = \int_0^{2\pi} \int_0^R [A + \chi \ln r] r \, dr \, d\phi \qquad (24)$$

where $F_D$ is the force resulting from integration of the measured normal-stress distribution. In all instances, $F_{rheo}$ agreed with $F_D$ to within the experimental error. For example, in one of the experiments with 1.49% PAA at $\dot{\gamma}$ up to 355 $s^{-1}$ in the 2° cone, the average difference between $F_{rheo}$ and $F_D$ was 4.2%; and, at the three highest shear rates, the difference was less than 2%. For the 7.3% PIB, the average difference was 2.9%.

Examples of the measured logarithmic stress distributions are given in Figure 6. For all shear rates, it should be noted that the pressure obtained by extrapolation to the platen rim was a positive quantity.

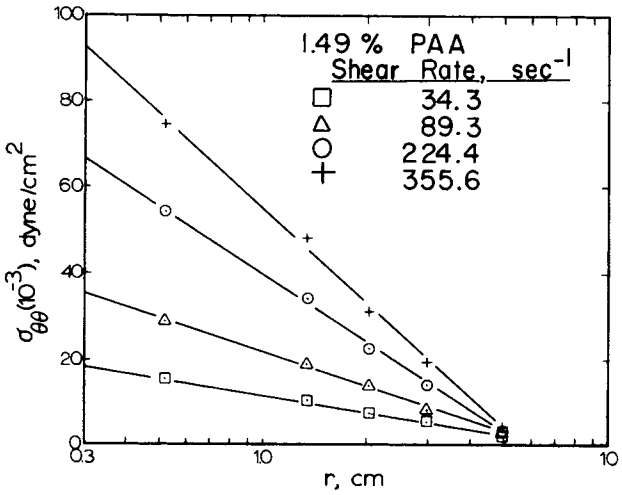


Fig. 6. Measured normal stress as a function of radial position for the 1.49% PAA solution at various shear rates.

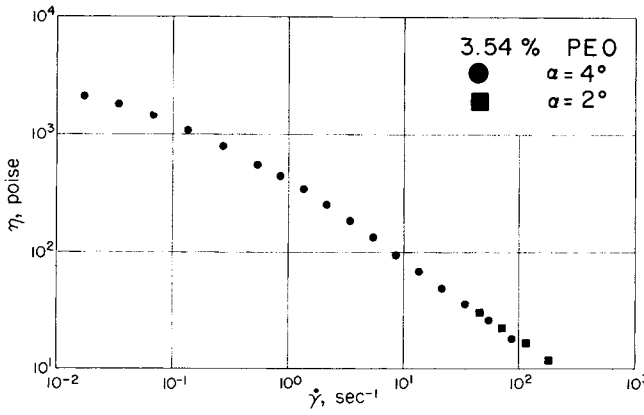


Fig. 7. Apparent viscosity as a function of shear rate for the 3.54% PEO solution.

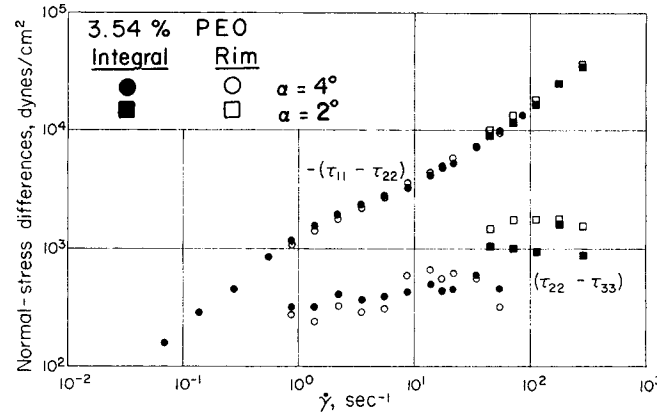


Fig. 8. Primary and secondary normal-stress differences as a function of shear rate for the 3.54% PEO solution.

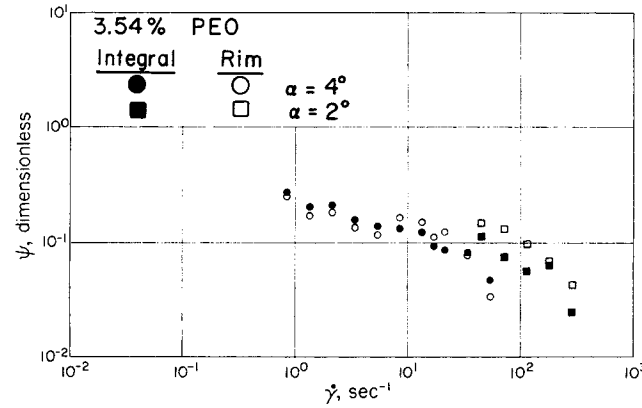


Fig. 9. Normal-stress-difference ratio as a function of shear rate for the 3.54% PEO solution.

The viscosity of the 1.49% polyacrylamide solution was higher than that of the 1.00% solution, as expected. However, an increase in concentration decreased the magnitude of the recoverable shear $S$ where

$$S \equiv \frac{\tau_{11} - \tau_{22}}{\tau_{21}} \qquad (25)$$

Equation (25) is commonly known as Hooke's law of shear (27, 28), and $S$ is the recoverable shear or shear strain.

This is consistent with the theoretical predictions of Flory (6):

$$\tau = \frac{RT\nu_e\gamma}{V} = RTC_e\gamma = \frac{k\gamma}{J_c}. \qquad (26)$$

The elastic compliance $J_c$ which is analogous to the shear strain $S$ is inversely proportional to the concentration.

The 1.00% Separan data were qualitatively similar to those of the more concentrated PAA solution (30).

A 3.54% PEO solution was analyzed in the same manner as the PAA solutions. The resulting data for the three rheological functions are presented in Figures 7 and 8. The majority of the data were in the non-Newtonian viscosity range, the lower shear-rate data approaching the lower Newtonian value. The ratio of the normal-stress differences $\psi$ was clearly determined to be a function of the shear rate as shown in Figure 9, similar to that of the PAA solutions. The values of $N_1$ for this PEO solution at a given shear rate are comparable with those of the 1.49% PAA solution. The shear-stress data at a given value of the

shear rate, however, are much larger than those of the PAA solution. Thus, values of the recoverable shear are smaller. Recoverable shear data are shown in Figure 10.

Two PIB solutions were tested to determine their rheological responses to viscometric shearing. The viscosity and normal-stress differences for the 7.30% PIB solution are shown in Figures 11 and 12, respectively, as a function of shear rate, while the normal-stress difference ratio is given in Figure 13. Similar functional relationships exist for the 4.17% PIB solution (*30*). Both solutions exhibited much smaller normal stresses than did the PAA and PEO solutions. The ratio $\psi$ for the 4.17% PIB solution appears to be constant (*30*); but the shear-rate range was small, and there was considerable uncertainty in the data since the normal stresses were relatively small. However, in the case of the 7.30%-PIB-solution data which were more accurate, the ratio $\psi$ is a function of the shear rate, Figure 13.

As with the PAA and PEO solutions, the PIB-solution normal-stress differences from the two methods of analysis were in agreement within the experimental error. Also, $F_{\text{rheo}}$ and $F_D$ were in good agreement.

## DISCUSSION

The experimental observations for viscosity and, especially, for normal forces may be adversely affected by misalignment of the cone and plate (*42*), by failure to maintain a spherical fluid-air interface (*1*), and by secondary flows (*10, 18, 19*) induced principally by the combined effects of the centrifugal-force field and elastic forces. In addition, the normal-force measurements are directly affected by the centrifugal-force field, by surface tension (*1*), and by imperfections and improper positioning of the transducers.

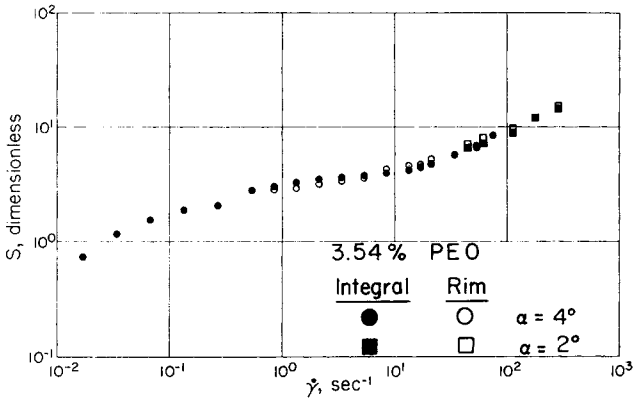


Fig. 10. Recoverable shear as a function of shear rate for the 3.54% PEO solution.

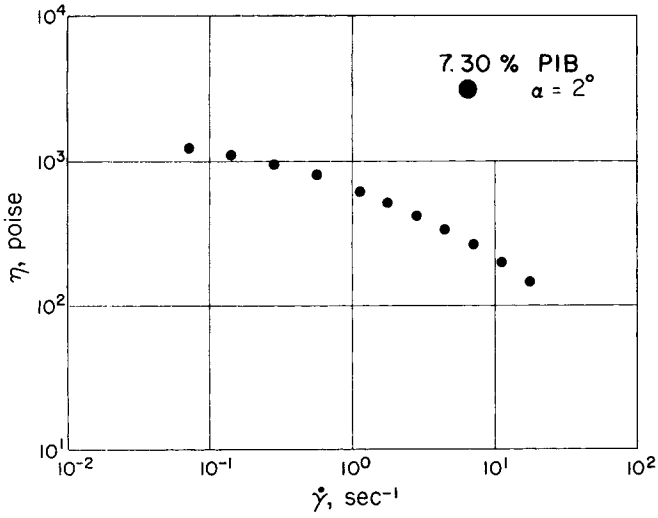


Fig. 11. Apparent viscosity as a function of shear rate for the 7.30% PIB solution.

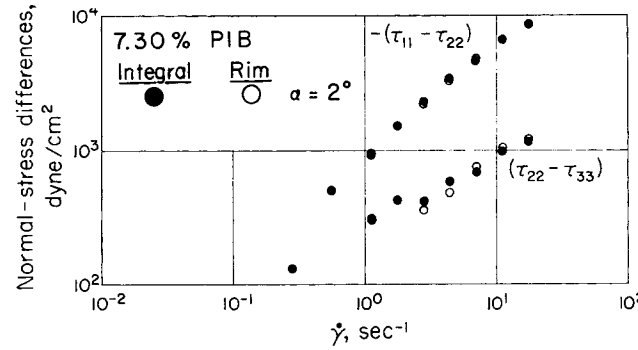


Fig. 12. Normal-stress differences as a function of shear rate for the 7.30% PIB solution.

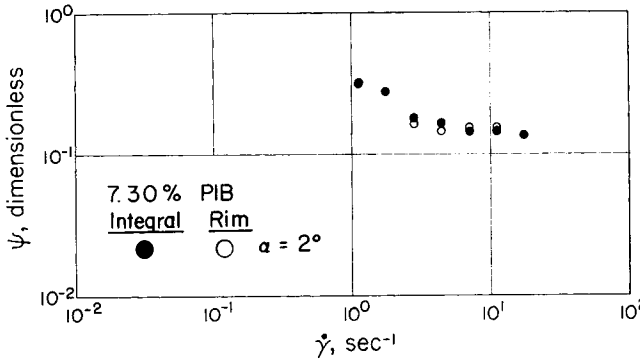


Fig. 13. Normal-stress-difference ratio as a function of shear rate for the 7.30% PIB solution.

The equations of motion require a more complicated velocity field than the simple viscometric flow represented by Equation (7) or the more accurate equation derived by Frederickson (*7*). The centrifugal-force field resulting from fluid rotation provides a potential for flow radially outward along the rotating platen, but the fluid elasticity generates a potential for flow radially inward along the rotating platen; thus, a viscoelastic fluid may have a less severe flow perturbation than an inelastic fluid. Flows having opposite directions of circulation have been reported for large cone angles (*10*). However, Hoppmann et al. (*18, 19*) have investigated the effect of the centrifugal-force field and elasticity on the flow field in a cone-and-plate shear generator and have demonstrated that for small cone angles (less than 10°) the flow perturbations resulting from the centrifugal force and fluid elasticity are very small. Furthermore, from theoretical estimates and experimentation, Kaye et al. (*25*) report that the effect of secondary flow on normal stresses is negligibly small, provided that small cone angles are used. Since satisfactory means for correcting for the effects of such flow have not been reported, one uses small cone angles (usually 4° or less) to reduce secondary flow.

The centrifugal-force field causes an apparent decrease in the measured value of the total normal force. A first-order experimental correction was determined for the effect of this centrifugal-force field by shearing an inelastic Newtonian fluid (an NBS viscometer calibrating oil). The total downward thrust $F_c$ is shown in Figure 14 as a func-

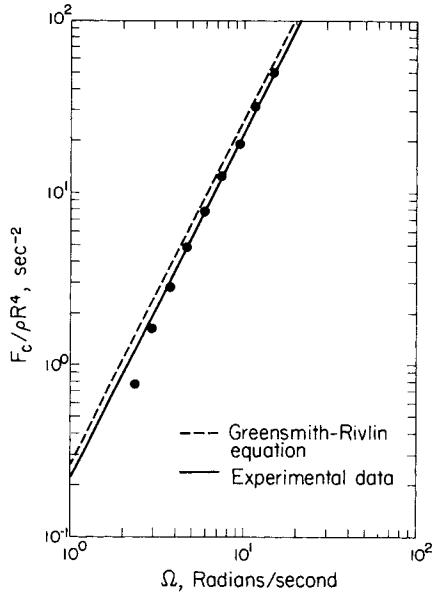


**Fig. 14. Inertial-force correction as a function of angular velocity of the rotating cone, obtained from the shear testing of an inelastic Newtonian fluid.**

tion of the angular velocity Ω. The experimental data were found to fit the equation

$$F_c = \frac{\rho \pi R^4 \Omega^{2.02}}{15.48} \tag{27}$$

Greensmith and Rivlin (*15*) have postulated the following equation based on semitheoretical considerations (shown in Figure 14):

$$F_c = \rho \pi R^4 \Omega^2/12. \tag{28}$$

Huppler et al. (*21*) have reported data for fluids of differing viscosity and density which support the Greensmith-Rivlin equation. The correction given by Equation (27) was applied to all total-thrust measurements reported. However, since the normal stresses generated by the fluids tested were relatively large, the inertial-force correction never exceeded 2.7% of the corrected total axial thrust.

The transducer responses are affected by transducer misalignment and structural imperfections in addition to the factors affecting the total normal force. Individual transducer corrections for these combined factors were determined as a function of the angular velocity of the cone in a manner similar to that for the total inertial-force correction (*30*). In the case of the 7.3% PIB solution, the average of the corrections was about 5.5%—the largest being those for the outer transducer, where the average was 15.3% and the maximum 24%. Many corrections for the other fluids were larger than these. Although these corrections are relatively large, the good agreement between $F_{\text{rheo}}$ and $F_D$ and the normal-stress differences—especially $N_2$ determined by the integral-force and rim-pressure methods, all at two different cone angles—implies that the results are relatively accurate.

Unusual care must be exercised to achieve and maintain the cone and plate near the ideal geometry. Prior to the shearing of a fluid sample, the cone and plate were adjusted within one micron of the desired axial position (elevation) at the center of the plate. However, deflections of the normal-force spring by the generated normal stresses permitted the plate to move upward from the position, resulting in small but measurable effects on the data. In a test with the 1.49% PAA solution (the most critical case), a 50-micron upward displacement of the plate from the desired position generated 4 and 8% decreases in the viscosity and normal thrust, respectively. Consequently, as equilibrium was approached, the cone was raised the distance required to compensate for deflection of the normal-force spring. For transient experimentation, a very stiff normal-force spring, a load cell, or a noncompliant stop must be used to reduce or eliminate axial motion of the plate. The cone and plate surfaces at the rim were adjusted to within three microns of the desired locations at regions near the adjustment studs. Deviations were sometimes greater at other locations. The data for the two directions of rotation were essentially the same—the maximum difference of 3% occurring at low velocities—which suggests that platen alignment was satisfactory.

The rim-pressure method is based on Equation (17), which is valid if the fluid-air interface is spherical and if the effects of surface tension and body forces are negligible. It is believed that adequate corrections for the centrifugal forces were made and that the surface-tension effects were sufficiently similar for static and dynamic conditions to be virtually eliminated by the use of static measurements as the reference. On the other hand, it is unlikely that the interface is ever exactly spherical, even for small cone angles, in consequence of the combined effects of the gravitational, centrifugal, and surface-tension forces and secondary flow. However, Kaye et al. (*25*) varied the shape of the interface for a 10-cm-diameter 3.1° cone from concave to convex (a radial variation of 1.1 mm) and found a maximum change of 6% in the total normal thrust. Using a 4° cone, we (*30*) varied the interface considerably outward and inward from an approximately spherical interface; the effect on the total and local normal forces appeared to be negligible. The good agreement of the data from the integral-force and rim-pressure methods suggests that the conditions of Equation (17) were satisfactorily met.

Vale et al. (*25*) determined normal-stress differences from cone-and-plate data by means of the the integral-force method, using total-normal-force data and stress-distribution data, the latter obtained from a transducer connected to the test fluid through a fluid-filled hole in a movable plate. They tested only one fluid, a solution of high-molecular-weight polyisobutene in a low-molecular-weight polyisobutene. The hole errors, which they determined as the difference between the pressure at $R$ and the secondary normal-stress difference from the integral-force method, were surprisingly large, about $-2(\tau_{21})$. They also report that a relationship involving the gradients of the normal pressure with plate radial distance for cone-and-plate and parallel-plate geometries and the gradients of $N_2$ and the hole error with $\dot{\gamma}$ was satisfied. Their results are in qualitative agreement with ours in that $N_2$ is finite and positive, though relatively small. Also, from their results, we computed $\psi$ to decrease from a value of about 0.08 to 0.09 at their lowest shear rates to about 0.04 at a shear rate of approximately 25 $s^{-1}$. However, their cone-and-plate instrumentation does not provide data for two independent assessments of $N_1$, $N_2$, and the total normal force. Also, their measurements may not be as responsive to transients and as free of certain errors as measurements made by means of the subject instrumentation.

## CONCLUSIONS

Although the principles involved in the analysis of the data are not original with this report, the instrumentation, which eliminates hole and other errors and some restric-

tions in the determination of the normal-stress differences, is new. The authors are unaware of any previous report of simultaneous single-geometry measurements of both the stress distribution and the total axial thrust having the potential of measurements made by use of our instrumentation. These measurements made possible for the first time the use of data from one experiment to make two independent assessments of the total normal thrust; two independent evaluations of $N_1$, the first normal-stress difference; and two independent evaluations of $N_2$, the second normal-stress difference. The data obtained in this study were not susceptible to many types of errors involved in previous investigations—such as errors induced by transmission of pressure by the test fluid through holes to the pressure sensor, those induced by the time required to reach equilibrium, those induced by yield stresses, or some induced by surface tension—nor were the results restricted by the implicit assumptions involved in a constitutive equation or in an integral inversion technique. The instrumentation is especially advantageous for transient measurements.

Although the accuracy of the secondary-normal-stress-difference determinations in particular was less than desired owing to imperfections of the available transducers, our results represent a definite improvement over most previous data and support the following conclusions:

1. The secondary normal-stress difference was finite for the shear rates investigated, indicating the invalidity of the Weissenberg hypothesis.
2. The magnitude of $N_2$ increased with the shear rate, except for some PEO and PAA data at the higher shear rates. At the lowest shear rates used, $N_2$ was up to ½ as large as the coexisting $N_1$. With one exception (the 4.17% PIB solution), $\psi$ decreased as the shear rate increased.
3. The sign of $N_2$ was positive; that is, represented a net compression.
4. The values of $N_1$ and $N_2$ calculated by means of the two methods of analysis were in good agreement. Therefore, it is concluded that the rim-pressure method of analysis can be used to predict the rheological stress state if care is exercised to establish and maintain the required boundary conditions.
5. A cone-and-plate (or parallel-plate) shearing device without a total-normal-thrust measuring system but having two or more small, sensitive pressure transducers appropriately located with the pressure sensors flush with the plate surface is a promising means for determining the complete stress state of a viscoelastic fluid. The effectiveness of the instrumentation will increase with the ongoing improvement in available transducers.


## ACKNOWLEDGMENT

The authors appreciate the fellowship and research-grant support provided by the National Science Foundation and the traineeship support provided by the National Aeronautics and Space Administration.


## NOTATION

$A$ = value of $\sigma_{22}$ at $r = 1$ cm, dynes/cm$^2$
$C_e$ = chain concentration, moles/cm$^3$
$F$ = axial thrust, defined by Equation (19), dynes
$F_c$ = inertial-force correction, dynes
$F_D$ = force resulting from integration of the measured normal-stress distribution, defined by Equation (24), dynes
$F_{\text{rheo}}$ = total axial thrust measured on the Rheogoniometer, dynes
$J_e$ = elastic compliance, cm$^2$/dyne
$k$ = coefficient in Equation (26), dimensionless
$N_1$ = primary normal-stress difference, $\tau_{11} - \tau_{22}$, dynes/cm$^2$
$N_2$ = secondary normal-stress difference, $\tau_{22} - \tau_{33}$, dynes/cm$^2$
$p$ = isotropic pressure, defined by Equation (3), dynes/cm$^2$
$p_A$ = ambient pressure, dynes/cm$^2$
$r$ = radial position in polar spherical coordinates, cm
$R$ = radius of the plate and the cone, cm
$R$ = Boltzmann constant per mole, erg/(mole °K)
$S$ = recoverable shear, or shear strain, defined by Equation (25), dimensionless
$T$ = absolute temperature, °K
$V$ = total volume of the system, cm$^3$
$V_i$ = $i^{\text{th}}$ component of the velocity vector, cm/s
$X_i$ = $i^{\text{th}}$ component of the position vector, cm

### Greek Letters

$\alpha$ = complementary cone angle, $\theta_c - \pi/2$, radians
$\gamma$ = shear strain, dimensionless
$\dot{\gamma}$ = shear rate, s$^{-1}$
$\Gamma$ = torque transmitted through the fluid, dyne-cm
$\delta_{ij}$ = unit tensor (Kronecker Delta)
$\eta$ = apparent viscosity, poise, g/(cm-s)
$\theta$ = colatitudinal angle in polar spherical coordinates, radians
$\theta_c$ = colatitudinal cone angle in polar spherical coordinates, radians
$\nu_e$ = effective number of moles of chains in a real network
$\rho$ = fluid density, g/cm$^3$
$\sigma_{ij}$ = total-stress tensor, dynes/cm$^2$
$\tau$ = shear stress, dynes/cm$^2$
$\tau_{ij}$ = shear-stress, or deviatoric-stress, tensor, dynes/cm$^2$
$\tau_{21}$ = shear stress, dynes/cm$^2$
$\tau_{11} - \tau_{22}$ = primary normal-stress difference, dynes/cm$^2$
$\tau_{22} - \tau_{33}$ = secondary normal-stress difference, dynes/cm$^2$
$\phi$ = azimuthal angle in polar spherical coordinates, radians
$\chi$ = slope of the measured radial stress distribution, defined by Equation (15), dynes/cm$^2$
$\psi$ = normal-stress-difference ratio, defined by Equation (22), dimensionless
$\Omega$ = angular velocity of the rotating cone, radians/s

### Subscripts

1 = orthogonal vector component designating the direction of flow
2 = orthogonal vector component designating the direction of the velocity gradient
3 = orthogonal vector component designating the neutral direction (normal to the 12 plane)
$i, j$ = indices, = 1, 2, 3
$\phi$ = in the $\phi$ direction

## LITERATURE CITED


1. Adams, N., and A. S. Lodge, *Phil. Trans. Roy. Soc. London*, **A256**, 149 (1964).
2. Bird, R. B., W. E. Stewart, and E. N. Lightfoot, "Transport Phenomena," Wiley, New York (1960).
3. Christiansen, E. B., and M. J. Miller, *Trans. Soc. Rheol.*, **15**, 189 (1971).
4. Denn, M. M., and J. J. Roisman, *AIChE J.*, **15**, 454 (1969).
5. Eyring, H., D. Henderson, B. J. Stover, and E. M. Eyring, "Statistical Mechanics and Dynamics," Wiley, New York (1964).
6. Flory, P. J., "Principles of Polymer Chemistry," Cornell

University Press, Ithaca, New York (1953).
7. Fredrickson, A. G., Ph.D. thesis, Univ. of Wisconsin, Madison (1959).
8. ———., "Principles and Applications of Rheology," Prentice-Hall, Englewood Cliffs, N. J. (1964).
9. Garner, F. H., A. H. Nissan, and G. F. Wood, *Phil. Trans. Roy. Soc. London*, **A243**, 37 (1950).
10. Giesekus, H., "Proc. of the Fourth Intern. Congress on Rheology, Vol. I," ed. by E. H. Lee, p. 249, Interscience, New York (1965).
11. Ginn, R. F., Master's thesis, Univ. of Delaware, Newark (1964).
12. ———., and M. M. Denn, *AIChE J.*, **15**, 450 (1969).
13. Ginn, R. F., and A. B. Metzner, "Proc. of Fourth Intern. Congress on Rheology, Part 2," ed. by E. H. Lee, p. 583, Interscience, New York (1965).
14. ———., *Trans. Soc. Rheol.*, **13**, 429 (1969).
15. Greensmith, H. W., and R. S. Rivlin, *Phil. Trans. Roy. Soc. London*, **A245**, 399 (1953).
16. Han, C. D., Paper K-5, 42nd Annual Meeting of Soc. of Rheology, Knoxville, Tennessee (1971).
17. Haynes, J. W., and R. I. Tanner, "Proc. of Fourth Intern. Congress on Rheology, Part 3," ed. by E. H. Lee, p. 389, Interscience, New York (1965).
18. Hoppmann, W. H., II, and C. N. Baronet, *Trans. Soc. Rheol.*, **9**, 417 (1965).
19. Hoppmann, W. H., II, and C. E. Miller, *ibid.*, **7**, 181 (1963).
20. Huppler, J. D., *ibid.*, **9**, 273 (1965).
21. ———., E. Ashare, and L. A. Holmes, *ibid.*, **11**, 159 (1967).
22. Jackson, R., and A. Kaye, *Brit. J. Appl. Phys.*, **17**, 1355 (1966).
23. Jobling, A., and J. E. Roberts, *J. Polymer Sci.*, **36**, 433 (1959).
24. ———., "Rheology, Theory and Applications, Vol. II," ed. by R. R. Eirich, Chapt. 13, p. 503, Academic Press, New York (1958).
25. Kaye, A., A. S. Lodge, and D. G. Vale, *Rheol. Acta*, **7**, 368 (1968).
26. Kotaka, T., M. Kurata, and M. Tamura, *J. Appl. Phys.*, **30**, 1705 (1959).
27. Lodge, A. S., "Elastic Liquids," Academic Press, New York (1964).
28. Markovitz, H., and D. Brown, *Trans. Soc. Rheol*, **7**, 37 (1963).
29. Miller, C. E., and W. H. Hoppmann II, "Proc. of Fourth Intern. Congress on Rheology, Part 2," ed. by E. H. Lee, p. 619, Interscience, New York (1965).
30. Miller, M. J., Ph.D. thesis, Univ. of Utah, Salt Lake City (1968).
31. Philippoff, W., *Trans. Soc. Rheol.*, **5**, 163 (1961).
32. ———, and R. A. Stratton, *ibid.*, **10**, 467 (1966).
33. Pollett, W. F. O., *Brit. J. Appl. Phys.*, **6**, 199 (1955).
34. Ree, F. H., T. Ree, and H. Eyring, *Ind. Eng. Chem.*, **50**, 1036 (1958).
35. Roberts, J. E. "Proc. of the Second Intern. Congress on Rheology," p. 91, Butterworths, London (1954).
36. Sakiadis, B. C., *AIChE J.*, **8**, 317 (1962).
37. Stevens, W. E., Ph.D. thesis, Univ. of Utah, Salt Lake City (1953).
38. Tanner, R. I., *Trans. Soc. Rheol.*, **11**, 347 (1967).
39. *Ibid.*, **14**, 483 (1970).
40. White, J. L., and A. B. Metzner, "Progr. in Intern. Research on Thermodynamic and Transport Properties," ed. by J. F. Masi and D. H. Tsai, p. 748, Academic Press, New York (1962).
41. Williams, M. C., *Chem. Eng. Sci.*, **20**, 693 (1965).
42. ———., *AIChE J.*, **11**, 467 (1965).

*Manuscript received November 16, 1969; revision received January 11, 1972; paper accepted January 13, 1972.*

# Kinetics of Anion Exchange Accompanied by Fast Irreversible Reaction

**E. E. GRAHAM and J. S. DRANOFF**

**Department of Chemical Engineering**
**Northwestern University, Evanston, Illinois 60201**

**The kinetics of binary anion exchange accompanied by a fast irreversible reaction at the exchanger surface was studied. Dowex 1, X-8, in the hydroxyl form was contacted with a strong acid in a well-stirred batch reactor and concentration-time data were obtained by electrical conductivity measurements. The process was analyzed assuming rate control by film diffusion, intraparticle diffusion, and a combination of both mechanisms. The results indicated that models based on the individual mechanisms gave quite satisfactory representations of the data under appropriate conditions, but the combined model appears superior in the nominally intraparticle diffusion controlled range. It was also found that severe particle cracking occurs, particularly with larger resin particles, at high solution concentrations. This results in degradation of the particles as well as apparent intraparticle diffusion coefficients that vary during the exchange process. Care must be taken to avoid or to account for this phenomenon.**

Recently Helfferich (*1*) has developed a detailed analysis of ion exchange coupled with chemical reaction based on the generally accepted model of the exchange process but modified to include the effects of reaction. This model considers the exchange process to be controlled by transport of ions to the exchange surface and/or diffusion of counter (exchanging) ions within the exchanger. The first step (film diffusion) is approximated as diffusion through an idealized thin stagnant film of thickness $\delta$. The second step (intraparticle diffusion) is considered to be diffusion of ions in a spherical, quasi-homogeneous exchanger matrix in which there is no co-ion uptake and no solvent flux.

Correspondence concerning this paper should be addressed to J. S. Dranoff. E. E. Graham is with Esso Research and Engineering Company, Florham Park, New Jersey.